ACADEMIC PRESS

Available online at www.sciencedirect.com

SCIENCE DIRECT®

Experimental Cell Research 291 (2003) 212–227

Experimental Cell Research

www.elsevier.com/locate/yexcr

Novel binding sites of 15-deoxy-$\Delta^{12,14}$-prostaglandin J_2 in plasma membranes from primary rat cortical neurons

Tatsurou Yagami,[a,b,*] Keiichi Ueda,[a] Kenji Asakura,[a] Nobuo Takasu,[a] Toshiyuki Sakaeda,[c] Naohiro Itoh,[a] Gaku Sakaguchi,[a] Junji Kishino,[a] Hitosi Nakazato,[a] Yoshihiko Katsuyama,[a] Tohru Nagasaki,[a] Noboru Okamura,[a] Yozo Hori,[a] Kohji Hanasaki,[a] Akinori Arimura,[a] and Masafumi Fujimoto[a]

[a] *Discovery Research Laboratories, Shionogi and Co., Ltd., 12-4, Sagisu 5-Choume, Fukushima-ku, Osaka 553-0002, Japan*
[b] *Department of Molecular Pharmacology and Neurobiology, Yokohama City University School of Medicine, Yokohama, Japan*
[c] *Department of Hospital Pharmacy, School of Medicine, Kobe University, Kobe, Japan*

Received 4 March 2003, revised version received 25 June 2003

Abstract

15-Deoxy-$\Delta^{12,14}$-prostaglandin J_2 (15d-$\Delta^{12,14}$-PGJ_2) is an endogenous ligand for a nuclear peroxysome proliferator activated receptor-γ (PPAR). We found novel binding sites of 15d-$\Delta^{12,14}$-PGJ_2 in the neuronal plasma membranes of the cerebral cortex. The binding sites of [^{3}H]15d-$\Delta^{12,14}$-PGJ_2 were displaced by 15d-$\Delta^{12,14}$-PGJ_2 with a half-maximal concentration of 1.6 μM. PGD_2 and its metabolites also inhibited the binding of [^{3}H]15d-$\Delta^{12,14}$-PGJ_2. Affinities for the novel binding sites were 15d-$\Delta^{12,14}$-PGJ_2 $>$ Δ^{12}-PGJ_2 $>$ PGJ_2 $>$ PGD_2. Other eicosanoids and PPAR agonists did not alter the binding of [^{3}H]15d-$\Delta^{12,14}$-PGJ_2. In primary cultures of rat cortical neurons, we examined the pathophysiologic roles of the novel binding sites. 15d-$\Delta^{12,14}$-PGJ_2 triggered neuronal cell death in a concentration-dependent manner, with a half-maximal concentration of 1.1 μM. The neurotoxic potency of PGD_2 and its metabolites was also 15d-$\Delta^{12,14}$-PGJ_2 $>$ Δ^{12}-PGJ_2 $>$ PGJ_2 $>$ PGD_2. The morphologic and ultrastructural characteristics of 15d-$\Delta^{12,14}$-PGJ_2-induced neuronal cell death were apoptotic, as evidenced by condensed chromatin and fragmented DNA. On the other hand, we detected little neurotoxicity of other eicosanoids and PPAR agonists. In conclusion, we demonstrated that novel binding sites of 15d-$\Delta^{12,14}$-PGJ_2 exist in the plasma membrane. The present study suggests that the novel binding sites might be involved in 15d-$\Delta^{12,14}$-PGJ_2-induced neuronal apoptosis.

Keywords: 15-Deoxy-$\Delta^{12,14}$-prostaglandin J_2; Prostaglandin D_2; Peroxysome proliferator-activated receptor-γ; Plasma membrane; Apoptosis; Neuron; Cerebral cortex; Alzheimer's disease; Stroke

Introduction

Eicosanoids, which are oxygenated metabolites of arachidonic acid (AA), modulate cellular function during a variety of physiologic and pathologic processes [1]. Eicosanoids are divided into two groups according to their mechanism of action: the conventional eicosanoids, e.g., prostaglandin D_2 (PGD_2), and the cyclopentenone-type PGs, e.g., 15-deoxy-$\Delta^{12,14}$-prostaglandin J_2 (15d-$\Delta^{12,14}$-PGJ_2). The conventional eicosanoids act on cell surface receptors to exert their action [2]. On the other hand, the cyclopentenone PGs are actively transported into cells and accumulate in the nucleus and thereby exert a wide variety of biological actions. One such effect is cell growth inhibition induced by blockage of cell cycle progression [3]. Thus, 15d-$\Delta^{12,14}$-PGJ_2 has been believed to lack cell surface receptors.

PGD_2 is metabolized to PGJ_2, Δ^{12}-PGJ_2, and 15d-$\Delta^{12,14}$-PGJ_2 in the presence of serum albumin [4]. Although the intracellular receptor of 15d-$\Delta^{12,14}$-PGJ_2 had not been reported, 15d-$\Delta^{12,14}$-PGJ_2 is an endogenous ligand for peroxysome proliferator-activated receptor-γ (PPAR) and is a

* Corresponding author. Fax: +81-45-785-3645.
E-mail address: VZX00556@nifty.com and yagami@pharmac.med.yokohama-cu.ac.jp (T. Yagami).

0014-4827/$ – see front matter © 2003 Elsevier Inc. All rights reserved.
doi:10.1016/S0014-4827(03)00369-0

weak activator of PPARα [5,6]. The PPARs belong to the nuclear receptor superfamily of ligand-dependent transcription factors. PPARγ is nominally expressed in hippocampal and cerebellar neurons [7], but it has not yet been detected in the cerebral cortex. On the other hand, PPARα is located in the nuclei of both neurons and glial cells in the cerebral cortex [8]. Recently, this nuclear receptor emerged from a role limited to lipid and glucose metabolism and adipocyte differentiation to a power player in the general transcription control of numerous cellular processes, with implications for cell cycle control, apoptosis, carcinogenesis, inflammation, atherosclerosis, and immunomodulation [9].

PPARγ agonists, including 15d-$\Delta^{12,14}$-PGJ_2, rescue cerebellar granule neurons from lipopolysaccharide-induced cell death in vivo [10]. On the contrary, 15d-$\Delta^{12,14}$-PGJ_2 induces cell death via apoptosis in primary cultures of rat cortical neurons and human neuroblastoma SH-SY5Y cells [11]. 15d-$\Delta^{12,14}$-PGJ_2 causes cleavage of poly (ADP-ribose) polymerase (PARP), a protein target for caspase [11]. The caspase inhibitor, Z-VAD, prevents the morphologic changes and the cleavage of PARP caused by 15d-$\Delta^{12,14}$-PGJ_2, indicating an involvement of caspase in 15d-$\Delta^{12,14}$-PGJ_2-mediated apoptosis [11]. However, they have not yet demonstrated that the apoptotic signals induced by 15d-$\Delta^{12,14}$-PGJ_2 are mediated through the binding to PPARγ. Collectively, these reports suggest that 15d-$\Delta^{12,14}$-PGJ_2 induces apoptosis independently of PPARγ. Actually, 15d-$\Delta^{12,14}$-PGJ_2 induces apoptosis via a novel mechanism involving reactive oxygen species and is unrelated to activation of PPARγ in hepatic myofibroblasts [12]. Moreover, 15d-$\Delta^{12,14}$-PGJ_2 inhibits the β_2 integrin-dependent production of reactive oxygen intermediates, suggesting its interaction with an unknown receptor on neutrophils distinct from PPARγ [14]. These PPAR-independent pathways suggest novel targets for 15d-$\Delta^{12,14}$-PGJ_2.

In the present study, we synthesized [^{3}H]15d-$\Delta^{12,14}$-PGJ_2 from [^{3}H]PGD_2 in serum-free medium. To ascertain whether novel targets of 15d-$\Delta^{12,14}$-PGJ_2 exist, we performed a binding assay of [^{3}H]15d-$\Delta^{12,14}$-PGJ_2 to plasma membranes of cortical neurons. Here, we provide the first evidence that ovel binding sites of 15d-$\Delta^{12,14}$-PGJ_2 exist on the neuronal cell surface. Furthermore, we evaluate the pathophysiologic roles of the novel binding site in primary cultures of cortical neurons and suggest a possible involvement of the novel binding sites in the 15d-$\Delta^{12,14}$-PGJ_2-induced apoptosis.

Materials and methods

Materials

Dulbecco's modified Eagle's medium, Leibovitz's L-15 medium, trypsin, deoxyribonuclease I, fetal bovine serum, horse serum, penicillin, and streptomycin were obtained from Gibco (Grand Island, NY). PGD_2, PGE_2, 9α-11β-PGF_2, $PGF_2\alpha$, PGI_2, PGJ_2, Δ^{12}-PGJ_2, 15d-$\Delta^{12,14}$-PGJ_2, LTB_4, LTC_4, and LTD_4 were purchased from Cascade Biochem Ltd. (Berkshire, UK). WY-14643 and clofibrate were purchased from Biomol Research Laboratories, Inc. (PA, USA). BRL-49653, Troglitazone, Pioglitazone, U-46619, a stable agonist for TXA_2 receptor, and BWA868C were synthesized in our laboratory. [^{3}H]PGD_2 (68 Ci/mmol) was purchased from Perkin–Elmer Life Science Products (Boston, MA). A glass fiber filter (GF/C) was obtained from Whatman (Maidstone, UK). Hoechst 33258 was purchased from Molecular Probes (Eugene, OR). A kit for the TUNEL assay was purchased from Boehringer Mannheim (Mannheim, Germany). All other chemicals were of reagent grade.

Preparation of [^{3}H]15d-$\Delta^{12,14}$-PGJ_2

[^{3}H]15d-$\Delta^{12,14}$-PGJ_2 was produced by treatment of [^{3}H]PGD_2 as follows. A solution of [^{3}H]PGD_2 (168 Ci/mmol, 42 μCi) in methanesulfonic acid:water (1:2) (0.5 ml) was stirred for 1 h at 50°C. The reaction mixture was poured into ice water (5 ml), extracted with ethyl acetate, washed with water and brine, and purified by preparative high-performance liquid chromatography (HPLC) to give [^{3}H]15d-$\Delta^{12,14}$-PGJ_2 (14 μCi, radiochemical purity 95.6%). The HPLC conditions were as follows: column: TSKgel ODS 80T_S 4.6 mm $\times$ 15 cm; mobile phase: CH_3CN:H_2O:AcOH = 55:45:0.03; flow rate: 1 ml/min; detector: UV = 210 nm; scintillator: ULTIMA FLO-M 1.5 ml/min for radioactivity; flow monitor: Packard 525TR; and retention time: 13 min. [^{3}H]15d-$\Delta^{12,14}$-PGJ_2 was identified with standard 15d-$\Delta^{12,14}$-PGJ_2 by thin liquid chromatography (TLC). The TLC conditions were as follows: plate: Silicagel (Merck KGF_{254}, solvent:chloroform methyl alcohol = 9:1, Rf = 0.4). Identification of [^{3}H]15d-$\Delta^{12,14}$-PGJ_2 was carried out by means of ultraviolet (UV) spectrometry of 15d-$\Delta^{12,14}$-PGJ_2. UV spectra were recorded by HPLC with a UV spectrometer (200–400 nm) and a Waters 990 photodiode array detector. The UV max was 308 nm. The specific radioactivity of [^{3}H]15d-$\Delta^{12,14}$-PGJ_2 was more than 10 Ci/mmol.

Preparation of [^{3}H]Δ^{12}-PGJ_2

[^{3}H]Δ^{12}-PGJ_2 was prepared by treatment of [^{3}H]PGD_2 as follows. A solution of [^{3}H]PGD_2 (NEN, Lot No. 3301-014, 168 Ci/mmol, 100 μCi) in human serum albumin–0.1 M phosphate buffer (5 mg/ml, pH 7.02) (0.5 ml) was allowed to stand for 2 days at 37°C. The reaction mixture was acidified to pH 3 with 0.1 M citric acid (0.5 ml) and extracted with ethyl acetate (4 ml $\times$ 2). The extracts were washed with water (1.5 ml $\times$ 2) and brine (1 ml), dried with sodium sulfate, and concentrated under reduced pressure. The concentrate was purified by preparative HPLC to give [^{3}H]Δ^{12}-PGJ_2 (17.3 μCi, radiochemical purity above 99.9%; specific radioactivity, more than 10 Ci/mmol). [^{3}H]Δ^{12}-PGJ_2 was identified with standard Δ^{12}-PGJ_2 by

cochromatography on TLC and HPLC and UV spectrometry. The conditions for TLC and HPLC were as follows: TLC: plate: Silicagel Merck KGF_{254}; solvent: benzene:ethyl acetate:acetic acid = 50:50:2, Rf = 0.28. HPLC: column: TSKgel ODS $80T_M$ 4.6 mm × 25 cm. Mobile phase: acetonitrile:water:acetic acid = 43:57:0.1; flow rate: 1 ml/min; detector: UV = 210 nm, Retention time: 20 min. UV spectra (UV max 248 nm) were recorded by HPLC with a UV spectrometer (Waters 990 photodiode array detector; UV: 190–400 nm). The radiochemical purity was determined by HPLC equipped with a radioactivity flow monitor (Packard 525TR).

Preparation of [^{3}H]PGJ$_2$

[^{3}H]PGJ$_2$ was prepared by treatment of [^{3}H]PGD$_2$ as follows. A solution of [^{3}H]PGD$_2$ (NEN, Lot No. 3301-014, 168 Ci/mmol, 100 μCi) in 0.1 M phosphate buffer (pH 7.02) (50 μl) was allowed to stand for 24 h at 37°C. The reaction mixture was subjected to preparative HPLC to give [^{3}H]PGJ$_2$ (4.59 μCi, radiochemical purity above 99%; specific radioactivity, more than 10 Ci/mmol). [^{3}H]PGJ$_2$ was identified with unlabeled standard PGJ$_2$ by cochromatography on TLC and HPLC. The conditions for TLC and HPLC were as follows. TLC: plate: Silicagel Merck KGF_{254}; solvent: benzene:ethyl acetate:acetic acid = 50:50:2; Rf = 0.25. HPLC: Column: TSKgel ODS $80T_M$ 4.6 mm × 25 cm, mobile phase: acetonitrile:water:acetic acid = 40:60:0.1; flow rate: 1 ml/min; detector: UV = 210 nm; retention time: 24 min. The radiochemical purity was determined by HPLC equipped with a radioactivity flow monitor (Packard 525TR).

Binding assay of [^{3}H]15d-$\Delta^{12,14}$-PGJ$_2$, [^{3}H]Δ^{12}-PGJ$_2$, and [^{3}H]PGJ$_2$

Plasma membranes were prepared from rat cortices (E19) as previously reported [14]. As a plasma membrane marker, 5′-nucleotidase activity was measured according to the method of Aronson et al. [15]. The purity of plasma membranes was 10–15 times as high as that of homogenates. The standard reaction mixture of [^{3}H]15d-$\Delta^{12,14}$-PGJ$_2$ contained 50 mM Tris–HCl buffer (pH 8.0), 100 mM NaCl, [^{3}H]15d-$\Delta^{12,14}$-PGJ$_2$, and plasma membranes (10 μg) in a total volume of 100 μl. Incubation was initiated by addition of the reaction mixture to platelets or cultured neurons and was carried out at 4°C for 24 h. We determined nonspecific binding by performing incubations with [^{3}H]15d-$\Delta^{12,14}$-PGJ$_2$ in the presence of 100 μM unlabeled 15d-$\Delta^{12,14}$-PGJ$_2$. The specific binding was calculated by subtraction of the nonspecific binding from the total binding. Binding assays of [^{3}H]Δ^{12}-PGJ$_2$ and [^{3}H]PGJ$_2$ were performed according to that of [^{3}H]15d-$\Delta^{12,14}$-PGJ$_2$. All values were expressed as means of duplicate or triplicate experiments.

Binding assay of [^{3}H]PGD$_2$

The preparation of platelet membranes and the binding assay of [^{3}H]PGD$_2$ were performed as described previously [16]. Briefly, frozen-thawed membranes (80 μg) were incubated with 5 nM [^{3}H]PGD$_2$ in the absence or presence of increasing concentrations of the compounds in the incubation buffer (50 mM Tris–HCl buffer, pH 7.4, containing 10 mM $MgCl_2$) for 90 min at 4°C or for 60 min at room temperature, respectively. Nonspecific binding was determined in the presence of 10 μM unlabeled PGD$_2$. The incubation was terminated by rapid vacuum filtration with use of a glass fiber filter and washed several times in ice-cold saline, and then the radioactivities retained on the filters were measured with a liquid scintillation counter. The inhibitory activity of the compounds against the [^{3}H]PGD$_2$ specific binding was evaluated by estimation of its half-maximal inhibitory concentration (IC_{50}) from each displacement curve.

Tissue cultures

Neuronal cell cultures were prepared from rat cerebral cortices [17]. Cerebral cortices were dissociated in isotonic buffer [18] with 4 mg/ml trypsin and 0.4 mg/ml deoxyribonuclease I. Cells were plated at a density of 2.5×10^5 cells/cm^2 on poly-L-lysine-coated dishes in conditioning medium, Leibovitz's L-15 medium supplemented with 5% fetal bovine serum, and 5% horse serum at 37°C in 5% CO_2 and 9% O_2. On day 1 after plating, cultures were treated with 0.1 μM arabinosylcytosine C. Cultures prepared by this method consisted of approximately 95% neurons and 5% astrocytes.

Analysis of cell survival

Neurons (2.5×10^5 cells/cm^2) were treated with 15d-$\Delta^{12,14}$-PGJ$_2$ or its related compounds at 37°C. The 3-(4,5-dimethylthiazol-2-yl)-2,5-diphenyl tetrazolium bromide dye (MTT) reduction assay was employed for assessment of neurotoxicity of PGD$_2$ and its metabolites as previously reported [19].

Fluoromicroscopic analysis

Assessment of chromatin condensation was performed as previously described [20,21]. Neurons (2.5×10^5 cells/cm^2) were treated with 10 μM PGD$_2$ or 1 μM 15d-$\Delta^{12,14}$-PGJ$_2$ at 37°C for 12 h. The culture medium was exchanged with phosphate-buffered saline containing 10 μM Hoechst 33258 fluorescent dye. Cells were incubated for 10 min at 37°C in the dark and washed with phosphate-buffered saline. Hoechst33258-positive cells were visualized by fluorescence microscopy (365 nm excitation and 420 nm emission). Stained nuclei were categorized as follows: (i) normal nuclei, homogeneously stained chromatin; (ii) intact nuclei

with condensed chromatin, crescent-shaped areas of condensed chromatin often located near the periphery of the nucleus; and (iii) fragmented nuclei, more than two condensed micronuclei within the area of a neuron.

In situ labeling of nuclear DNA fragments

Neurons (2.5×10^5 cells/cm^2) were treated with 10 μM PGD_2 or 1 μM 15d-$\Delta^{12,14}$-PGJ_2 at 37°C for 12 h. Cortical cell cultures were stained by the TdT-mediated dUTP-biotin nick end-labeling (TUNEL) technique as described [22]. Apoptotic cells could be distinguished morphologically from necrotic cells by the presence of condensed brown nuclei.

Transmission electron microscopy

Ultrastructure of neurons was analyzed as previously [23]. Neurons (2.5×10^5 cells/cm^2) were treated with 10 μM PGD_2 or 1 μM 15d-$\Delta^{12,14}$-PGJ_2 at 37°C for 12 h. Cells were fixed in situ with 2.5% glutaraldehyde in phosphate buffer at 4°C for 2 h, and postfixed with 1% osmium tetroxide at 4°C. To increase contrast, cells were double-fixed with saturated thiocarbohydrazide-osmium. Samples were dehydrated in a graded series of ethanols and embedded in Epon 812. Ultrathin sections cut on a Reichert ultramicrotome were stained with uranyl acetate and lead citrate and were examined with a JOEL JEM 1200EX electron microscope.

Metabolism of [^{3}H]PGD_2

[^{3}H]PGD_2 was incubated in serum-free culture medium at 37°C. At the indicated times, samples were withdrawn, acidified to pH 3 with formic acid, and extracted immediately with ethyl acetate. The solvent was evaporated under nitrogen, and residual metabolites of [^{3}H]PGD_2 were converted quantitatively into naphthacyl ester by reaction with α-bromoacetonaphtone and diisopropylethylamine in acetonitrile. The acetonitrile was evaporated, and the residue was reconstituted in the chromatographic mobile phase containing glyceryl guiacholate, an internal standard for quantitation.

Statistical analysis

Data are given as means ± SEM (n = number of observations). Data were analyzed statistically by use of Student's nonpaired t test for comparison with the control group, and data on various inhibitors and blocker groups were analyzed statistically by use of two-way ANOVA followed by Dunnett's test for comparison with the PG group [24]. A half-maximal effective concentration (EC_{50}) and IC_{50} values were calculated by Microsoft Excel Fit as previously reported [25].

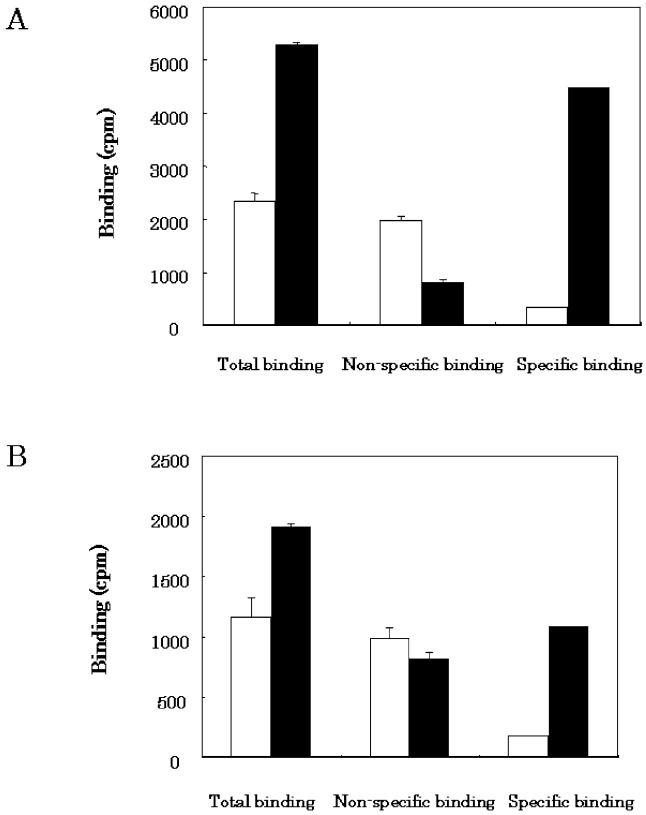

Fig. 1. (A) Binding assay of [^{3}H]PGD_2 and [^{3}H]15d-$\Delta^{12,14}$-PGJ_2. Plasma membranes from neurons (20 μg protein) were incubated with 10 nM [^{3}H]PGD_2 (open columns) or 10 nM [^{3}H]15d-$\Delta^{12,14}$-PGJ_2 (closed columns) at 4°C for 24 h. Total and nonspecific bindings of [^{3}H]PGD_2 or [^{3}H]15d-$\Delta^{12,14}$-PGJ_2 were measured in the absence and presence of 100 μM PGD_2 or 100 μM 15d-$\Delta^{12,14}$-PGJ_2, respectively. The specific bindings were calculated from the differences between total and nonspecific bindings. (B) Binding assay of [^{3}H]PGD_2: Neurons (open columns) or platelets (closed columns) were incubated with 5 nM [^{3}H]PGD_2 at 25°C for 1 h. Total and nonspecific bindings of [^{3}H]PGD_2 were measured in the absence and presence of 100 μM PGD_2, respectively. The specific bindings were calculated from the differences between total and nonspecific bindings.

Results

Binding assay of [^{3}H]15d-$\Delta^{12,14}$-PGJ_2 and [^{3}H]PGD_2 on neuronal membranes

A binding assay of [^{3}H]15d-$\Delta^{12,14}$-PGJ_2 to the plasma membranes (10 μg) was performed at 4°C for 24 h. Specific binding of [^{3}H]15d-$\Delta^{12,14}$-PGJ_2 was more than 80%, whereas that of [^{3}H]PGD_2 was less than 20% (Fig. 1A). PGD_2 receptor is expressed in various peripheral tissues, including platelets [26,27]. It may be difficult to detect PGD_2 receptor at low temperature. Therefore, we performed the binding assay of [^{3}H]PGD_2 under more optimal conditions at a higher temperature. As previously reported [16], we confirmed the specific binding sites of [^{3}H]PGD_2 in platelets by incubation at 25°C for 1 h (Fig. 1B). Nonspecific binding was measured at 100 μM PGD_2, and the specific binding consisted 57.0% of total binding in plate-

lets. However, few binding sites of PGD_2 have been detected in the cerebral cortex, whereas the specific binding of PGD_2 is highest in the pituitary gland, followed by the hypothalamus and the olfactory bulb of the rat brain [28]. We observed that nonspecific binding of [^{3}H]PGD_2 consisted of 84.3% of the total binding, and we confirmed that there were few specific binding sites of [^{3}H]PGD_2 in the cerebral cortex (Fig. 1B). Thus, novel binding sites of [^{3}H]15d-$\Delta^{12,14}$-PGJ_2 were detected in plasma membranes under conditions different from the optimal one for [^{3}H]PGD_2 binding.

Effect of temperature on binding of [^{3}H]15d-$\Delta^{12,14}$-PGJ_2 to plasma membranes

We examined the effect of temperature on the binding of [^{3}H]15d-$\Delta^{12,14}$-PGJ_2 to plasma membranes of rat cortical neurons (Fig. 2A). The ratio of specific binding of [^{3}H]15d-$\Delta^{12,14}$-PG J_2 to the total binding was 76.2% for incubation at 25°C for 1 h. The total binding of [^{3}H]15d-$\Delta^{12,14}$-PG J_2 for incubation at 25°C for 24 h was 3.1 times as high as that for 1 h. The ratio of its specific binding at 25°C for 24 h (47%) was lower than that at 25°C for 1 h (76%). On the other hand, the total binding of [^{3}H]15d-$\Delta^{12,14}$-PGJ_2 for incubation at 4°C for 1 h was reduced to half of that at 25°C for 1 h (Fig. 2A). The ratio of specific binding of [^{3}H]15d-$\Delta^{12,14}$-PG J_2 to the total binding at 4°C for 1 h (37%) was lower than that at 25°C for 1 h (76%). However, the total binding of [^{3}H]15d-$\Delta^{12,14}$-PGJ_2 for incubation at 4°C for 24 h was 18.2 times as large as that at 4°C for 1 h. In addition, the ratio of specific binding of [^{3}H]15d-$\Delta^{12,14}$-PGJ_2 to the total binding at 4°C for 24 h (87%) was higher than that at 4°C for 1 h (37%). Thus, incubation of [^{3}H]15d-$\Delta^{12,14}$-PGJ_2 at 4°C was optimal.

Effect of time and protein concentration on binding of [^{3}H]15d-$\Delta^{12,14}$-PGJ_2 to plasma membranes

We examined the time dependence of [^{3}H]15d-$\Delta^{12,14}$-PGJ_2 binding to plasma membranes. Incubation at 4°C increased the specific binding of [^{3}H]15d-$\Delta^{12,14}$-PGJ_2, and it reached a plateau at 16 h (Fig. 2B).

Next, we examined the dependence of the protein concentration on the binding assay of [^{3}H]15d-$\Delta^{12,14}$-PGJ_2 to plasma membranes at 4°C for 24 h. At 20 μg, total binding, nonspecific binding, and specific binding were increased linearly (Fig. 3A). Thus, incubation of [^{3}H]15d-$\Delta^{12,14}$-PGJ_2 with 10 μg plasma membranes at 4°C for 24 h was optimal.

Effect of 15d-$\Delta^{12,14}$-PGJ_2-related compounds on binding of [^{3}H]15d-$\Delta^{12,14}$-PGJ_2 to plasma membranes

We investigated the inhibitory effects of 15d-$\Delta^{12,14}$-PGJ_2-related compounds on the binding of 10 nM [^{3}H]15d-$\Delta^{12,14}$-PGJ_2 to plasma membranes (Fig. 3B). At 10 μM, their inhibitory effect was 15d-$\Delta^{12,14}$-PGJ_2 > Δ^{12}-PGJ_2 > PGJ_2 ≫ PGD_2 in sequence. In addition to 15d-$\Delta^{12,14}$-PGJ_2 and its precursors, PGA_2 significantly displaced the binding of [^{3}H]15d-$\Delta^{12,14}$-PGJ_2. On the other hand, IC_{50} values of PGE_2, LTB_4, and BWA868C, a PGD_2 receptor blocker, were above 100 μM. Thus, 15d-$\Delta^{12,14}$-PGJ_2 inhibited the binding of [^{3}H]15d-$\Delta^{12,14}$-PGJ_2 to plasma membranes most potently among 15d-$\Delta^{12,14}$-PGJ_2-related compounds.

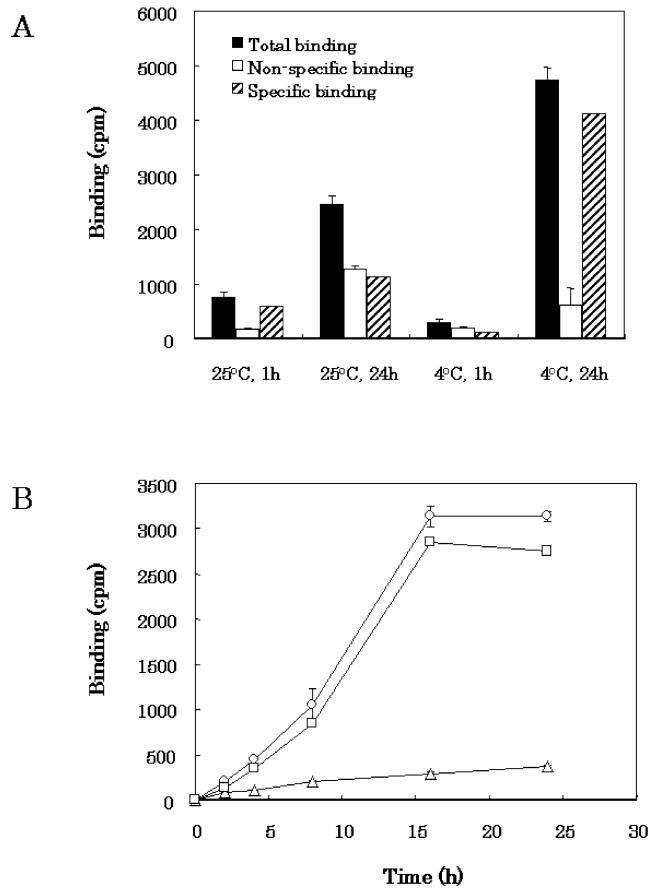

Fig. 2. Effect of temperature and time on the binding of [^{3}H]15d-$\Delta^{12,14}$-PGJ_2 to plasma membranes. (A) Temperature: Plasma membranes from neurons (20 μg protein) were incubated at 25° or 4°C for 1 or 24 h. Total binding (closed columns) and nonspecific bindings (open columns) of 10 nM [^{3}H]15d-$\Delta^{12,14}$-PGJ_2 were measured in the absence and presence of 100 μM 15d-$\Delta^{12,14}$-PGJ_2, respectively. The specific binding (hatched columns) was calculated from the differences between total and nonspecific binding. (B) Time: Plasma membranes from neurons (10 μg protein) were incubated at 4°C for 1–24 h. Total (circles) and nonspecific (triangles) bindings of 10 nM [^{3}H]15d-$\Delta^{12,14}$-PGJ_2 were measured in the absence and presence of 100 μM 15d-$\Delta^{12,14}$-PGJ_2, respectively. The specific binding (squares) were calculated from the differences between total and nonspecific bindings.

Effect of 15d-$\Delta^{12,14}$-PGJ_2 on binding of [^{3}H]15d-$\Delta^{12,14}$-PGJ_2 to plasma membranes

We investigated the effects of 15d-$\Delta^{12,14}$-PGJ_2 on [^{3}H]15d-$\Delta^{12,14}$-PGJ_2 binding to plasma membranes (10 μg) at 4°C for 24 h (Fig. 4A). 15d-$\Delta^{12,14}$-PGJ_2 inhibited the

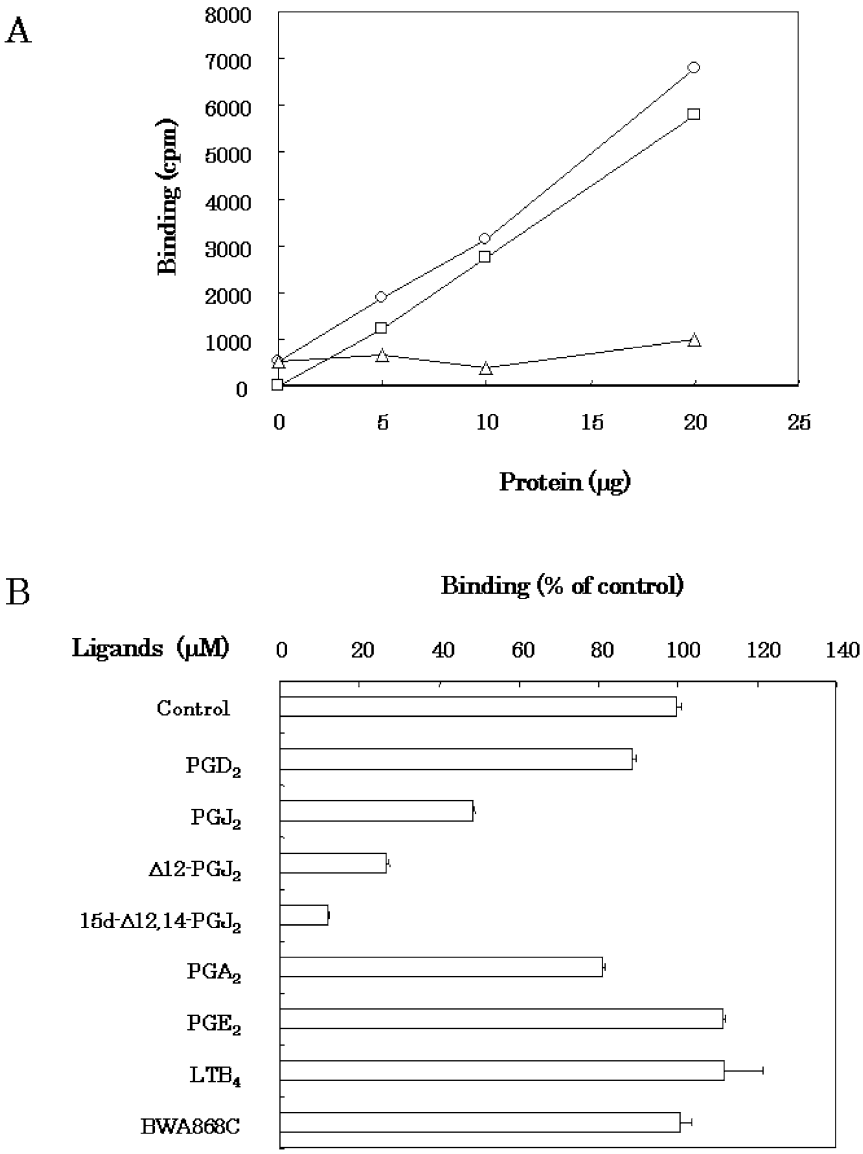

Fig. 3. Effect of protein and 15d-$\Delta^{12,14}$-PGJ_2-related compounds on the binding of [^{3}H]15d-$\Delta^{12,14}$-PGJ_2 to plasma membranes. (A) Protein: Plasma membranes from neurons were incubated at 4°C for 24 h at the indicated protein concentrations. Total binding (circles) and nonspecific bindings (triangles) of 10 nM [^{3}H]15d-$\Delta^{12,14}$-PGJ_2 were measured in the absence and presence of 100 μM 15d-$\Delta^{12,14}$-PGJ_2, respectively. The specific binding (squares) was calculated from the differences between total and nonspecific binding. (B) 15d-$\Delta^{12,14}$-PG J_2-related compounds: Plasma membranes from neurons (10 μg protein) were incubated with 10 nM [^{3}H]15d-$\Delta^{12,14}$-PGJ_2 at 4°C for 24 h in the presence of PGD_2, PGJ_2, Δ^{12}-PGJ_2, 15d-$\Delta^{12,14}$-PGJ_2, PGA_2, PGE_2, LTB_4, or BWA868C at 10 μM. The control value of [^{3}H]15d-$\Delta^{12,14}$-PGJ_2 binding was 2522.8 cpm.

specific binding of [^{3}H]15d-$\Delta^{12,14}$-PGJ_2 in a concentration-dependent manner, and its IC_{50} value was 1.6 μM. By Hill plot, a pseudo-Hill coefficient was 0.622 (Fig. 4B). Thus, 15d-$\Delta^{12,14}$-PGJ_2 appeared to recognize binding sites with different affinities in plasma membranes.

Concentration dependence of [^{3}H]15d-$\Delta^{12,14}$-PGJ_2 on binding to plasma membranes

We examined the concentration dependence of [^{3}H]15d-$\Delta^{12,14}$-PGJ_2 on the binding to plasma membranes of rat cortical neurons (Fig. 5A). At the indicated concentrations, [^{3}H]15d-$\Delta^{12,14}$-PGJ_2 was incubated with plasma membranes (10 μg) at 4°C for 24 h. [^{3}H]15d-$\Delta^{12,14}$-PGJ_2 bound to plasma membranes in a concentration-dependent manner, shown as a saturation curve. On the other hand, nonspecific binding of [^{3}H]15d-$\Delta^{12,14}$-PG J_2 in the presence of 100 μM 15d-$\Delta^{12,14}$-PGJ_2 occurred in proportion to its concentration. The specific binding of [^{3}H]15d-$\Delta^{12,14}$-PGJ_2 consisted of more than 80% of the total binding at any concentration. Although the specific binding increased in a concentration-dependent manner, it did not reach the saturation shown in Fig. 5A. Because a concentration of [^{3}H]15d-$\Delta^{12,14}$-PGJ_2 higher than 40 nM could not be prepared by the present

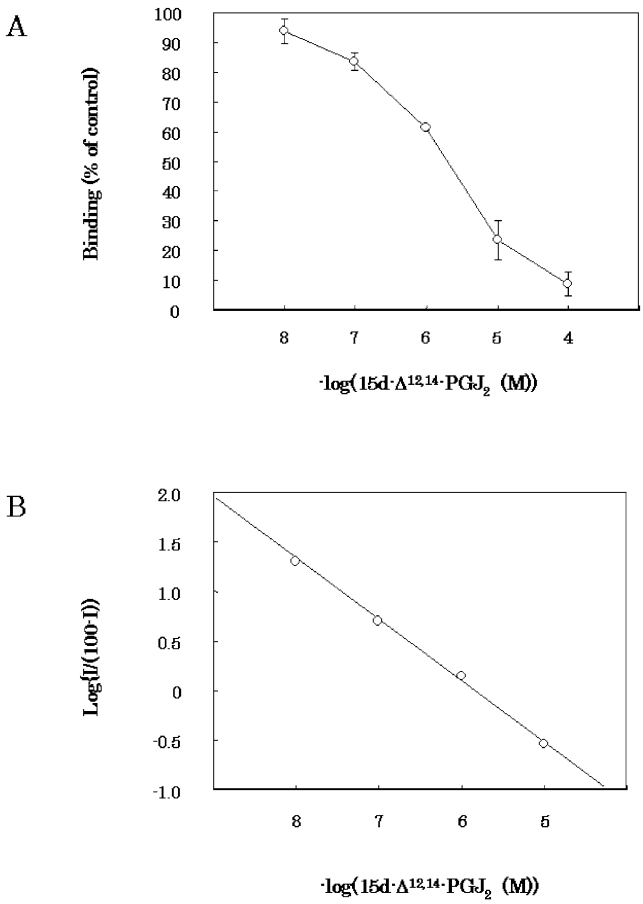

Fig. 4. Effect of 15d-$\Delta^{12,14}$-PG J_2 on the binding of [^{3}H]15d-$\Delta^{12,14}$-PG J_2 to plasma membranes. (A) 15d-$\Delta^{12,14}$-PGJ_2: Plasma membranes from neurons (10 μg protein) were incubated with 10 nM [^{3}H]15d-$\Delta^{12,14}$-PGJ_2 at 4°C for 24 h in the presence of 15d-$\Delta^{12,14}$-PGJ_2 at the indicated concentrations. (B) Hill plot: Data of (A) were analyzed by the pseudo-Hill plot.

synthesis method, a pseudo-Scatchard analysis was performed (Fig. 5B). Pseudovalues of B_{max} and K_d were 30.2 pmol/mg protein and 16.5 nM.

Inhibitory effects of 15d-$\Delta^{12,14}$-PGJ_2 precursors on specific binding sites of [^{3}H]PGJ_2 and [^{3}H]Δ^{12}-PGJ_2

We investigated the inhibitory effects of 15d-$\Delta^{12,14}$-PGJ_2 precursors on the binding of 10 nM [^{3}H]PGJ_2 (Fig. 6A) and 10 nM [^{3}H]Δ^{12}-PGJ_2 (Fig. 6B) to plasma membranes. 15d-$\Delta^{12,14}$-PGJ_2, Δ^{12}-PGJ_2, and PGJ_2 inhibited the specific binding of [^{3}H]PGJ_2 and [^{3}H]Δ^{12}-PGJ_2 in a concentration-dependent manner. Their inhibitory effects on the specific binding of [^{3}H]PGJ_2 and [^{3}H]Δ^{12}-PGJ_2 were 15d-$\Delta^{12,14}$-PGJ_2 > Δ^{12}-PGJ_2 > PGJ_2 in sequence. PGD_2 had little effect on the specific binding of [^{3}H]PGJ_2 and [^{3}H]Δ^{12}-PGJ_2. Thus, both [^{3}H]PGJ_2 and [^{3}H]Δ^{12}-PGJ_2 recognized the specific binding sites of [^{3}H]15d-$\Delta^{12,14}$-PGJ_2 in plasma membranes.

Effects of 15d-$\Delta^{12,14}$-PGJ_2 and its precursors on neuronal cell survival

Primary cultures of dissociated cortical neurons were exposed to 15d-$\Delta^{12,14}$-PGJ_2 and its precursors, and neuronal cell death was quantified at the indicated times after exposure (Fig. 7A). As well as 15d-$\Delta^{12,14}$-PGJ_2, PGD_2, PGJ_2, and Δ^{12}-PGJ_2 also killed neurons within 8 h (Fig. 7A). Among them, 15d-$\Delta^{12,14}$-PGJ_2 caused neuronal cell death most rapidly, and Δ^{12}-PGJ_2, PGJ_2, and PGD_2 did so in sequence. PGD_2 required a latent time to induce neuronal cell death (Fig. 7A). As shown in Fig. 5B, 15d-$\Delta^{12,14}$-PGJ_2 caused neuronal cell death in a concentration-dependent manner (EC_{50} = 1.1 μM). The EC_{50} of PGD_2 (>10 μM) was higher than that of 15d-$\Delta^{12,14}$-PGJ_2 (Fig. 7B). Thus, the potency of their neurotoxicity was 15d-$\Delta^{12,14}$-PGJ_2 > Δ^{12}-PGJ_2 > PGJ_2 > PGD_2.

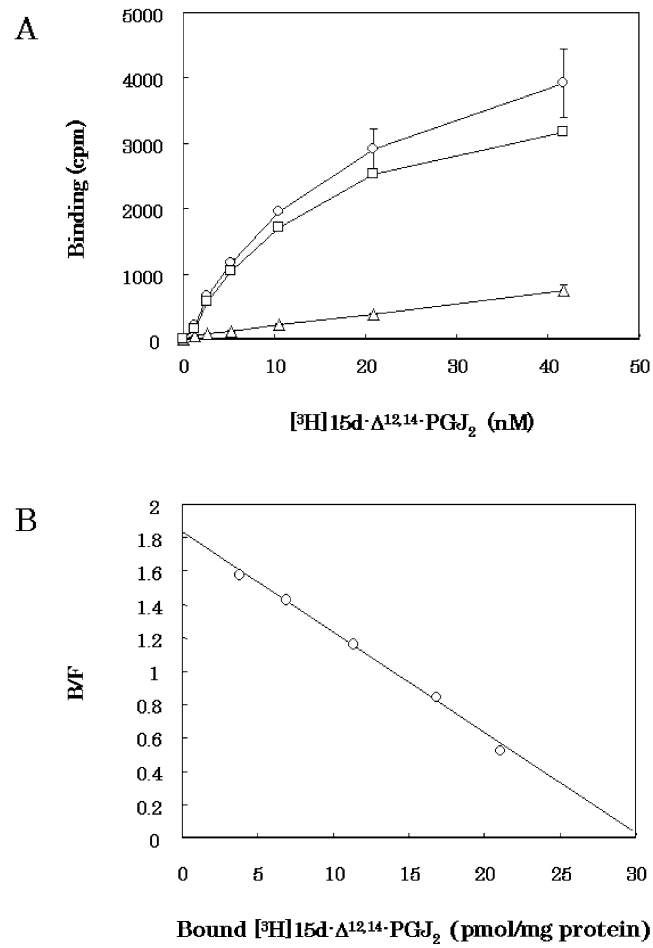

Fig. 5. Concentration dependency of [^{3}H]15d-$\Delta^{12,14}$-PGJ_2 on the binding to plasma membranes. (A) Ligand dependence: Plasma membranes from neurons (10 μg protein) were incubated with [^{3}H]15d-$\Delta^{12,14}$-PGJ_2 (1.25–40 nM) at 4°C for 24 h. Total (circles) and nonspecific (triangles) bindings of [^{3}H]15d-$\Delta^{12,14}$-PGJ_2 were measured in the absence and presence of 100 μM 15d-$\Delta^{12,14}$-PGJ_2, respectively. The specific bindings (squares) were calculated from the differences between total and nonspecific bindings. (B) Scatchard analysis: Data of A were analyzed by the Scatchard plot.

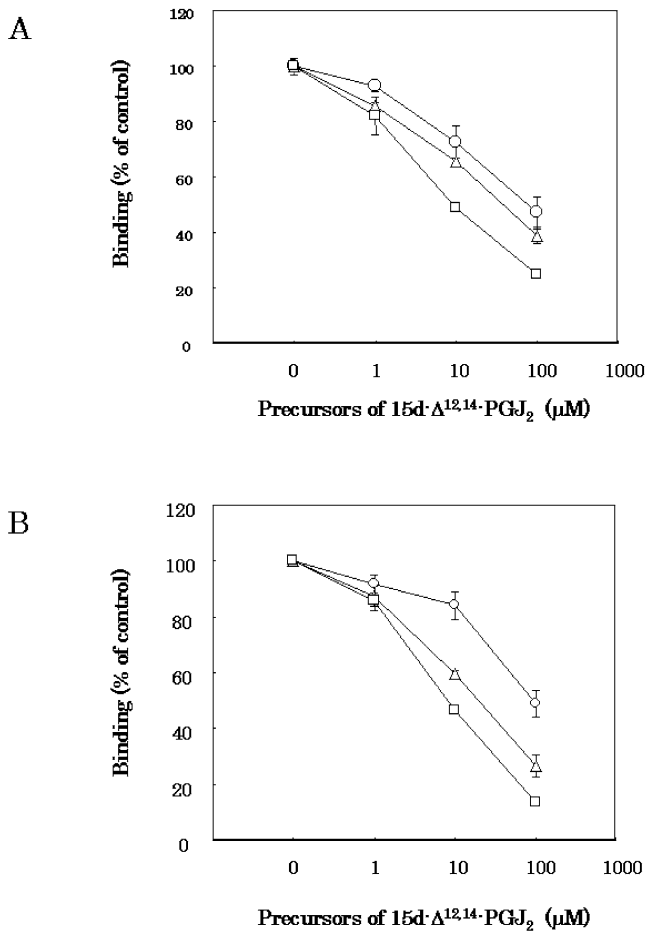

Fig. 6. Inhibitory effects of 15d-$\Delta^{12,14}$-PG J_2 precursors on specific binding sites of [^{3}H]PGJ_2 and [^{3}H]Δ^{12}-PGJ_2. Plasma membranes from neurons (10 μg protein) were incubated with PGJ_2 (open circles), Δ^{12}-PGJ_2 (open triangles), or 15d-$\Delta^{12,14}$-PGJ_2 (open squares) at the indicated concentrations in the presence of 10 nM [^{3}H]PGJ_2 (A) or 10 nM [^{3}H]Δ^{12}-PGJ_2 (B) at 4°C for 24 h. Control values of [^{3}H]PGJ_2 and [^{3}H]Δ^{12}-PGJ_2 binding were 1798 and 6021 cpm, respectively.

Effects of 15d-$\Delta^{12,14}$-PGJ_2-related compounds on cortical neuronal cell survival and specific binding of [^{3}H] 15d-$\Delta^{12,14}$-PGJ_2 to plasma membranes

Primary cultures of dissociated cortical neurons were exposed to 15d-$\Delta^{12,14}$-PGJ_2-related compounds, and neuronal cell death was quantified 24 h later (Fig. 8A). 15d-$\Delta^{12,14}$-PGJ_2 is known to be an endogenous ligand for PPARγ. However, PPARγ activators such as BRL-49653, troglitazone, and pioglitazone did not kill neurons at 10 μM. Although 15d-$\Delta^{12,14}$-PGJ_2 is also known to be a weak ligand for PPARα, PPARα activators such as WY-14643 and clofibrate had no effect on cell survival (Fig. 8A). Thus, 15d-$\Delta^{12,14}$-PGJ_2 induced neuronal cell death independently of PPARγ and PPARα.

Next, we examined inhibitory effects of PPARα activators and PPARγ activators on the specific binding of [^{3}H]15d-$\Delta^{12,14}$-PGJ_2 to plasma membranes (Fig. 8B). Neither PPARα activators nor PPARγ activators bound the specific binding sites of [^{3}H]15d-$\Delta^{12,14}$-PGJ_2. Thus, the specific binding sites of [^{3}H]15d-$\Delta^{12,14}$-PGJ_2 in the plasma membrane was distinguished from PPARα and PPARγ in the nucleus.

Effects of eicosanoids on neuronal survival

Primary cultures of dissociated cortical neurons were exposed to eicosanoids, and neuronal cell death was quantified 48 h later (Fig. 9). PGD_2 and PGA_2 exhibited neurotoxicity at 10 μM, whereas other eicosanoids such as PGE_2, 9α-11β-PGF_2, $PGF_2\alpha$, PGI_2, U-46619, LTC_4, and LTD_4 had no effect on neuronal cell survival (Fig. 9A). An endogenous PPARα agonist, LTB_4, also exhibited neurotoxicity (Fig. 9A). The neurotoxicity of PGD_2 was not suppressed by BWA868C, a PGD_2 receptor blocker (Fig. 9B).

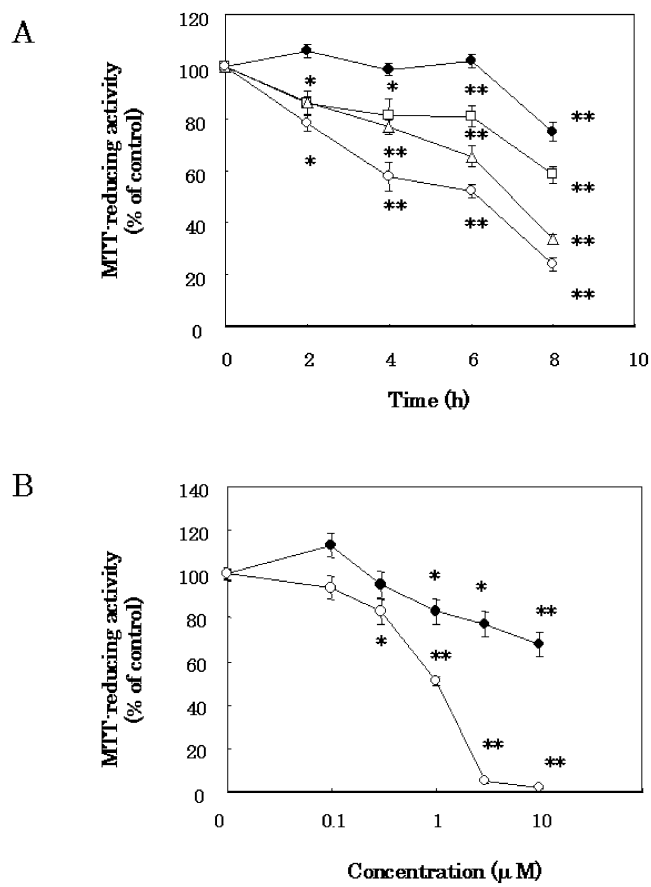

Fig. 7. Effects of 15d-$\Delta^{12,14}$-PGJ_2 and its precursors on neuronal cell survival. (A) Time course: Cortical neurons were treated with serum-free medium containing PGD_2 (closed circles), PGJ_2 (open squares), Δ^{12}-PGJ_2 (open triangles), or 15d-$\Delta^{12,14}$-PGJ_2 (open circles) at 10 μM. MTT-reducing activity was determined at the indicated time points after PGs treatment. (B) Dose response: Cortical neurons were treated with serum-free medium containing PGD_2 (closed circles) or 15d-$\Delta^{12,14}$-PGJ_2 (open circles) at the indicated concentrations. MTT-reducing activity was determined 24 h later. Data are expressed as means ± SEM ($n = 4$). *$P < 0.05$, **$P < 0.01$, compared with control by ANOVA followed by Dunnett's test.

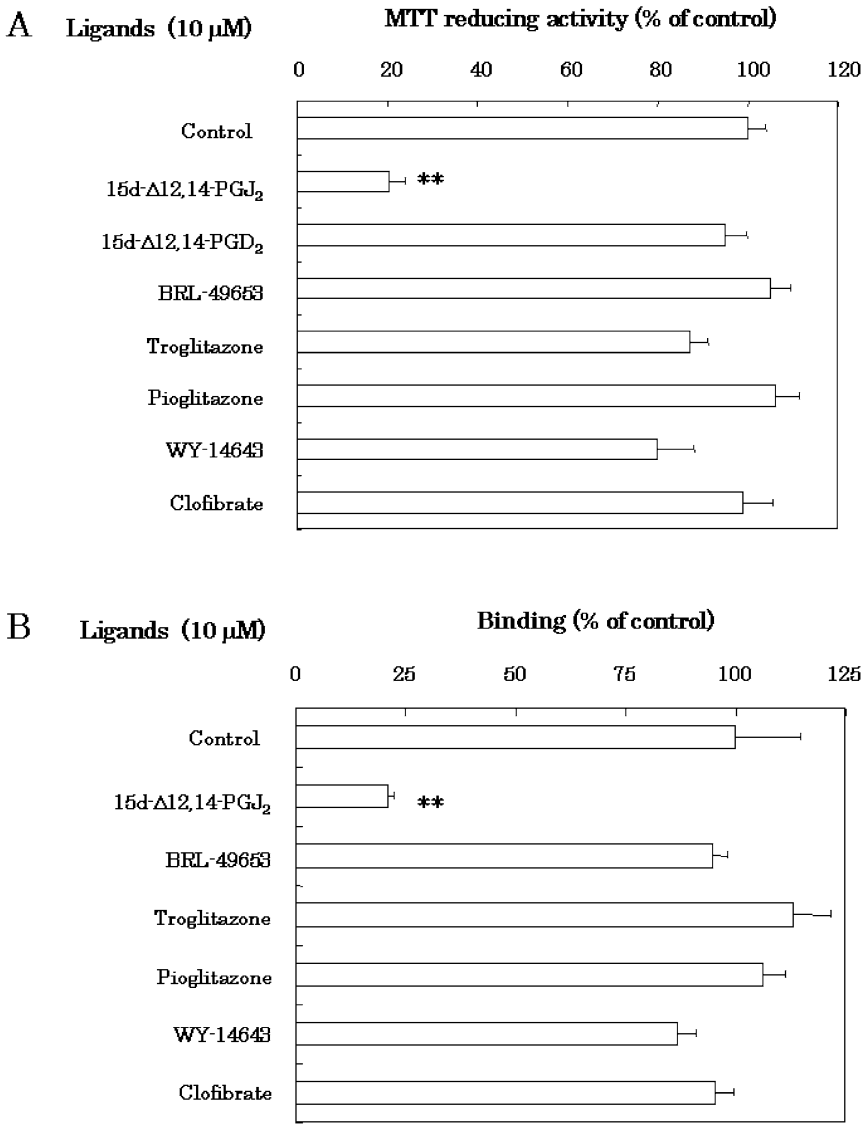

Fig. 8. Effects of PGD_2 metabolites and PPARγ activators on neuronal cell survival and on the binding of [^{3}H]15d-$\Delta^{12,14}$-PG J_2 to plasma membranes. (A) MTT assay: Rat cortical neurons were treated with 10 μM PGD_2 metabolites and PPARγ activators. MTT-reducing activity was determined 24 h later. Data are expressed as means ± SEM ($n = 4$). $^{**}P < 0.01$, compared with control by ANOVA followed by Dunnett's test. (B) Binding assay: Plasma membranes from neurons (10 μg protein) were incubated with 10 nM [^{3}H]15d-$\Delta^{12,14}$-PGJ_2 at 4°C for 24 h in the presence of 10 μM PGD_2 metabolites and PPARγ activators. The control value of [^{3}H]15d-$\Delta^{12,14}$-PGJ_2 binding was 2522.8 cpm.

Thus, there was a close correlation between the neurotoxicity of eicosanoids and the affinity of eicosanoids to the specific binding sites of [^{3}H]15d-$\Delta^{12,14}$-PGJ_2.

Morphologic changes in PG-treated neurons

In control cultures, examination of neurons by light microscopy showed extended neurites and smooth, round cell bodies (Fig. 10A). On the other hand, 15d-$\Delta^{12,14}$-PGJ_2-treated neurons showed some disruption of neurites. Some cell bodies shrank and lost their bright phase-contrast appearance at 24 h (Fig. 10B). Neurons treated with PGD_2 showed a similar disruption of neurites (Fig. 10C). The morphologic disruption in PGD_2-treated neurons was not suppressed by BWA868C (Fig. 10D). Thus, the morphologic changes in PGD_2-treated neurons were similar to those in 15d-$\Delta^{12,14}$-PGJ_2-treated ones, but were not ascribed to the activation of PGD_2 receptor.

Apoptotic features of PGD_2- and 15d-$\Delta^{12,14}$-PGJ_2-treated neurons

We studied the condensation of chromatin, a characteristic feature of apoptosis, in neurons (Figs. 11 and 12). PG-treated neurons were stained with Hoechst 33258 fluorescent dye (Fig. 11A–C). In untreated cultures, cells showed little fluorescence in the nucleus (Fig. 11A). On the other hand, condensed and fragmented chromatin was

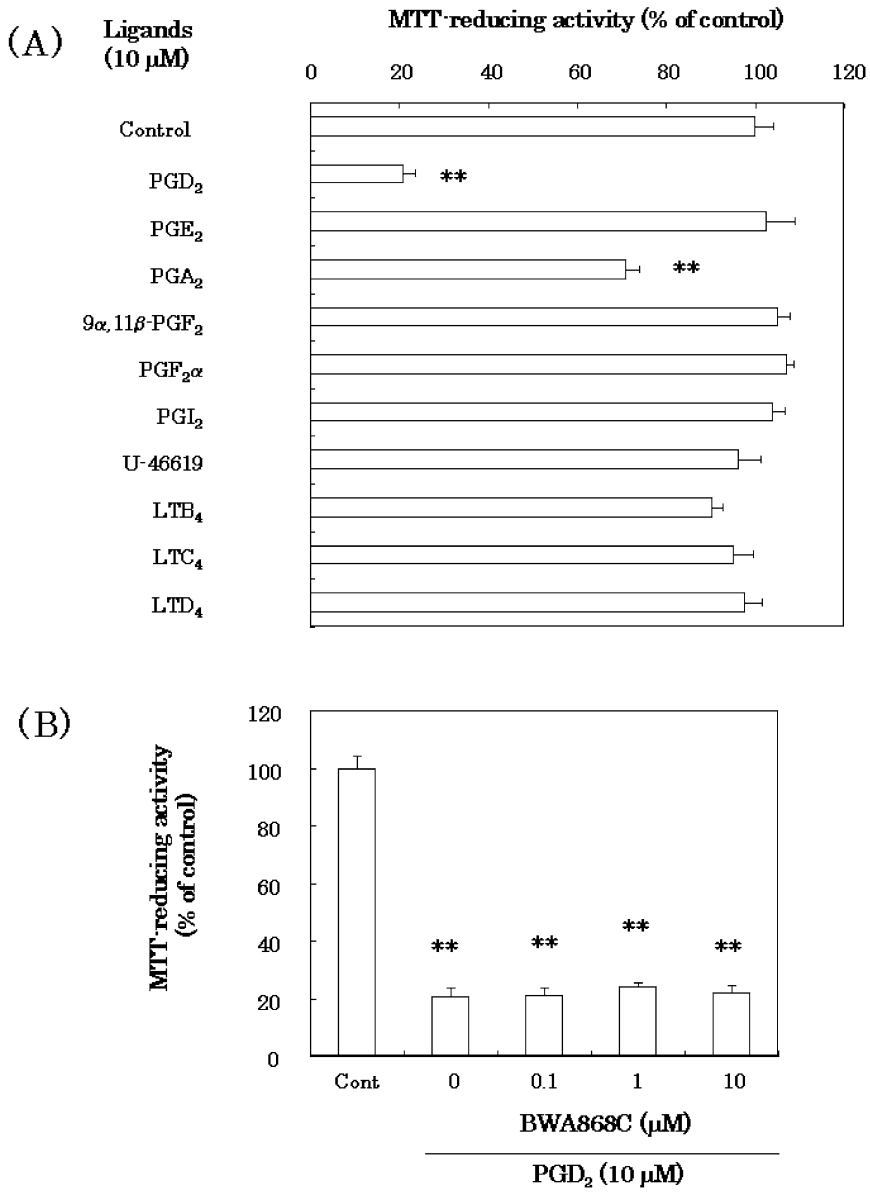

Fig. 9. Effects of eicosanoids on neuronal cell survival. (A) Cortical neurons were treated with various eicosanoids at 10 μM. (B) Effects of BWA868C on PGD_2-induced neuronal cell death. Cortical neurons were treated with BWA868C at the indicated concentrations in the presence of 10 μM PGD_2. MTT-reducing activity was determined 48 h later. Data are expressed as means ± SEM values ($n = 4$). $^{**}P < 0.01$, compared with control by ANOVA followed by Dunnett's test.

clearly observed in PGD_2- (Fig. 11B) and 15d-$\Delta^{12,14}$-PGJ_2-treated cultures (Fig. 11C). The number of nuclei that contained condensation or fragmentation of chromatin was increased in PGD_2- and 15d-$\Delta^{12,14}$-PGJ_2-treated neurons as compared to untreated controls (Fig. 12).

We also studied another apoptotic feature, fragmentation of DNA (Fig. 11D–F). With the TUNEL technique, it is possible to discriminate morphologically between the apoptotic nuclei by the presence of strand breaks in the DNA and the nonapoptotic nuclei by labeling of the nicked ends of DNA. After neurons were incubated without (Fig. 11D) or with PGD_2 (Fig. 11E) and 15d-$\Delta^{12,14}$-PGJ_2 (Fig. 11F) for 12 h, the number of TUNEL-positive nuclei was increased in PGD_2- and 15d-$\Delta^{12,14}$-PGJ_2-treated neurons as compared to untreated controls (Fig. 12). Thus, both PGD_2 and 15d-$\Delta^{12,14}$-PGJ_2 caused apoptotic features in cortical neurons.

Ultrastructural changes of PGD_2- and 15d-$\Delta^{12,14}$-PGJ_2-treated neurons

Neurons were incubated with vehicle (Fig. 13A), PGD_2 (Fig. 13B), or 15d-$\Delta^{12,14}$-PGJ_2 (Fig. 13C) for 18 h. On analysis by electron microscopy, the morphology of vehicle-treated neurons was healthy at 18 h (Fig. 13A). On the other hand, PGD_2- and 15d-$\Delta^{12,14}$-PGJ_2-treated neurons

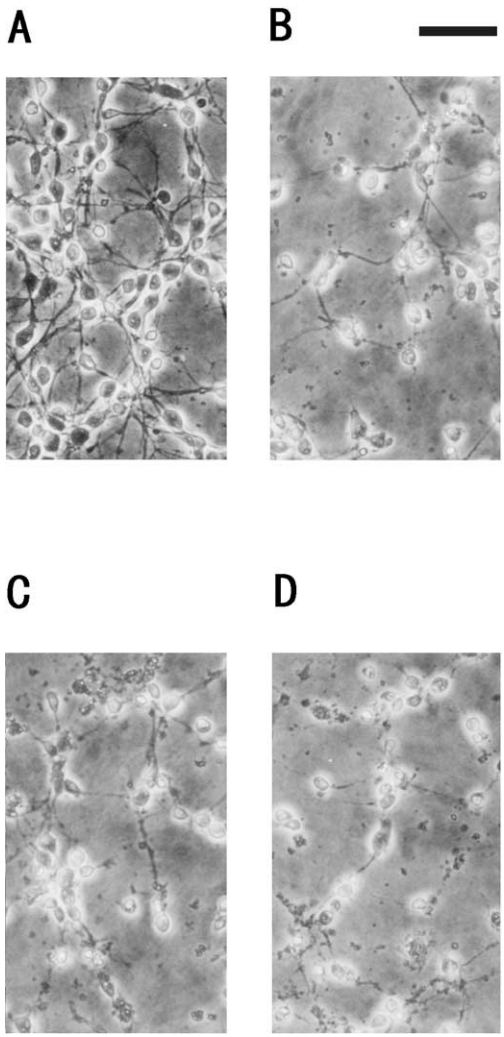

Fig. 10. Morphologic changes in PG-treated neurons. Cortical neurons were treated with vehicle (A), 10 μM PGD_2 (B), 10 μM PGD_2 + 10 μM BWA868C (C), or 10 μM 15d-$\Delta^{12,14}$-PGJ_2 (D). Neurons were examined by phase-contrast microscopy 24 h later. Bar = 100 μm.

showed characteristics of apoptosis (Fig. 13B and C). The neuronal size decreased progressively throughout the stages of cell death discussed below. In the early stage of PG-treated neuronal cell death, the plasma membrane became difficult to resolve, whereas features in the cytosol and the nucleus were unaltered. In the PGD_2-treated neurons, microtubules, neurofilaments, and ribosomes appeared condensed as the neurons continued to shrink. Moreover, decrease of the rough endoplasmic reticulum and progressive swelling of the Golgi cisterna were observed within the cytoplasm. The nucleus shrank progressively, and chromatin clumps became increasingly electron-dense. In the 15d-$\Delta^{12,14}$-PGJ_2-treated neurons, intracellular organelles such as the endoplasmic reticulum and the Golgi apparatus were lost, but the mitochondria remained intact. Condensation and fragmentation of chromatin were noted in the nucleus (Fig. 13B). Finally, the dying cells fragmented into small pieces. Thus, both PGD_2 and 15d-$\Delta^{12,14}$-PGJ_2 caused apoptosis in cortical neurons.

Nonenzymatic reaction from PGD_2 to 15d-$\Delta^{12,14}$-PGJ_2

PGD_2 is dehydrated to PGJ_2 in aqueous solution [29], and metabolized to 15-deoxy-$\Delta^{12,14}$-PGD_2 (15d-$\Delta^{12,14}$-PGD_2), Δ^{12}-PGJ_2, and 15d-$\Delta^{12,14}$-PGJ_2 in the presence of human albumin [4]. Therefore, we examined how [^{3}H]PGD_2 was metabolized in serum-free culture medium during incubation at 37°C (Fig. 14). The content of [^{3}H]PGD_2 was decreased to 20% at 41 h and to 0% within 160 h. Second, the content of [^{3}H]PGJ_2 was increased sharply, reached a peak (40.8%) at 17 h, and then decreased to 0% within 160 h. Third, the contents of [^{3}H]Δ^{12}-PGJ_2 and [^{3}H]15d-$\Delta^{12,14}$-PGJ_2 were persistently increased to 40 and 45%, respectively, during incubation. Finally, that of [^{3}H]15d-$\Delta^{12,14}$-PGD_2 was increased slightly, reached a plateau (10%), and stayed at that level during incubation. Thus, [^{3}H]PGD_2 was nonenzymatically metabolized to [^{3}H]15d-$\Delta^{12,14}$-PGD_2, [^{3}H]PGJ_2, [^{3}H]Δ^{12}-PGJ_2, and [^{3}H]15d-$\Delta^{12,14}$-PGJ_2 in serum-free culture medium.

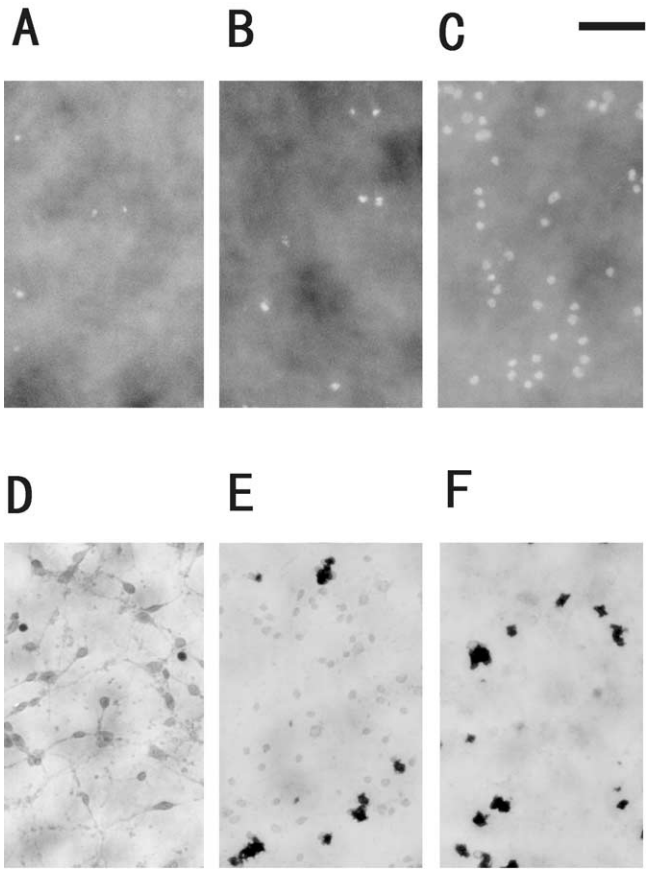

Fig. 11. Apoptotic features of PG-treated neurons. Cortical neurons were treated with control (A and D), 10 μM PGD_2 (B and E), or 10 μM 15d-$\Delta^{12,14}$-PGJ_2 (C and F). Neurons were stained with 1 μM Hoechst 33258 for 10 min 12 h later (A, B, and C). Neurons were fixed with 4% paraformaldehyde, washed twice with PBS, and stained by the TUNEL technique 12 h later (D, E, and F). Bar = 100 μm.

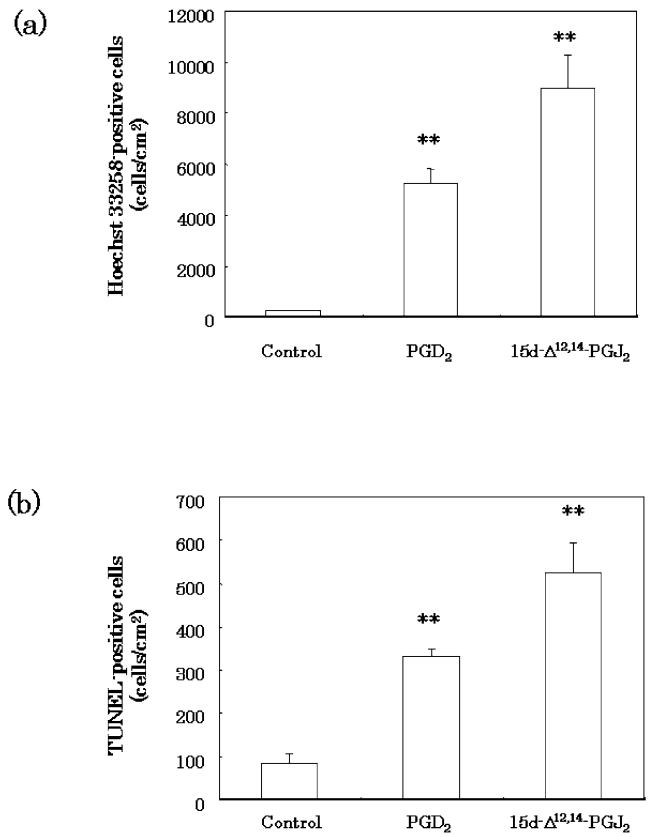

Fig. 12. 15d-$\Delta^{12,14}$-PGJ_2-induced apoptosis. Cortical neurons were treated with control (0.1% ethanol), 10 μM PGD_2, or 10 μM 15d-$\Delta^{12,14}$-PGJ_2. (a) Hoechst33258- and (b) TUNEL-positive neurons were detected 12 h later. Data are expressed as means ± SEM values (n = 4). $^{**}P < 0.01$, compared with control by ANOVA followed by Dunnett's test.

Discussion

In the present study, we found the novel binding sites of 15d-$\Delta^{12,14}$-PGJ_2 in the plasma membrane distinct from a nuclear receptor, PPARγ. The novel binding sites appear to be associated with 15d-$\Delta^{12,14}$-PGJ_2-induced apoptosis. To our knowledge, this is the first report on the cell surface binding sites of 15d-$\Delta^{12,14}$-PGJ_2.

Recently, it has been reported that 15d-$\Delta^{12,14}$-PGJ_2 induces neuronal apoptosis in primary cultures of rat cortical neurons [11]. In the present study, we confirmed that 15d-$\Delta^{12,14}$-PGJ_2-treated neurons exhibited apoptotic features such as condensed chromatin and fragmented DNA. PGJs are identified as natural ligands for PPARγ and were found to promote adipocyte differentiation [5,6]. 15d-$\Delta^{12,14}$-PGJ_2 induced neuronal apoptosis via PPARγ [11]. However, neuronal expression of PPARγ has not yet been detected in the cerebral cortex. No neurotoxicity of PPARγ agonists was detected in primary cultures of cortical neurons. Moreover, nonsteroidal anti-inflammatory drugs with PPARγ agonistic effects reduce apoptosis in cerebellar granule cells [31]. 15d-$\Delta^{12,14}$-PGJ_2 induced apoptosis in cortical neurons independently of PPARγ activation.

The cyclopentenone PGs have been believed to lack cell surface receptors. However, we found novel binding sites of 15d-$\Delta^{12,14}$-PGJ_2 in plasma membranes of cortical neurons. The affinity for the binding site was 15d-$\Delta^{12,14}$-PGJ_2 > Δ^{12}-PGJ_2 > PGJ_2 ≫ PGD_2. Furthermore, we detected the binding sites of 15d-$\Delta^{12,14}$-PGJ_2 precursors in plasma membranes by using [^{3}H]PGJ_2, and [^{3}H]Δ^{12}-PGJ_2. 15d-$\Delta^{12,14}$-PGJ_2, Δ^{12}-PGJ_2, and PGJ_2 inhibited the specific binding of [^{3}H]PGJ_2 and [^{3}H]Δ^{12}-PGJ_2 in a concentration-dependent manner. The inhibitory effects of PGD_2 metabolites on the binding sites of [^{3}H]PGJ_2 and [^{3}H]Δ^{12}-PGJ_2 were 15d-$\Delta^{12,14}$-PGJ_2 > Δ^{12}-PGJ_2 > PGJ_2 ≫ PGD_2, in the same sequence as those to the binding sites of [^{3}H]15d-$\Delta^{12,14}$-PGJ_2. Thus, PGJ_2 and Δ^{12}-PGJ_2 also appeared to recognize the same binding sites of 15d-$\Delta^{12,14}$-PGJ_2 in plasma membranes.

What type of pathophysiologic roles do the binding sites of 15d-$\Delta^{12,14}$-PGJ_2 play? 15d-$\Delta^{12,14}$-PGJ_2 induced neuronal cell death via apoptosis. The neurotoxic potency was 15d-$\Delta^{12,14}$-PGJ_2 > Δ^{12}-PGJ_2 > PGJ_2 ≫ PGD_2, in the same sequence as the affinity for the novel binding sites. Another cyclopentenone PG, PGA_2, also exhibited an affinity for the binding sites of 15d-$\Delta^{12,14}$-PGJ_2 and neurotoxicity. None of the other eicosanoids, PPAR agonists, or a PGD_2 receptor blocker exhibited any affinity for the binding sites and the neurotoxicity. The affinity of eicosanoids for the binding sites closely paralleled their neurotoxicity, suggesting involvement of the novel binding sites in neuronal cell death. To test the possibility, we performed binding assays of [^{3}H]15d-$\Delta^{12,14}$-PGJ_2 in various cells. We found the novel binding site of [^{3}H]15d-$\Delta^{12,14}$-PGJ_2 in the plasma membrane of bronchial smooth muscle cells. The inhibitory effects of 15d-$\Delta^{12,14}$-PGJ_2 precursors to the binding site was 15d-$\Delta^{12,14}$-PGJ_2 > Δ^{12}-PGJ_2 > PGJ_2 ≫ PGD_2, in the same sequence as for neurons. Toxic effects of 15d-$\Delta^{12,14}$-PGJ_2 precursors were 15d-$\Delta^{12,14}$-PGJ_2 > Δ^{12}-PGJ_2 > PGJ_2 ≫ PGD_2, in the same sequence as for neurons. Thus, one of the pathologic roles of 15d-$\Delta^{12,14}$-PGJ_2 was cell toxicity.

In a competition experiment, the IC_{50} of 15d-$\Delta^{12,14}$-PGJ_2 to the binding sites of [^{3}H]15d-$\Delta^{12,14}$-PGJ_2 was 1.6 μM. On the other hand, the apparent K_d value of [^{3}H]15d-$\Delta^{12,14}$-PGJ_2 was 16.5 nM by Scatchard analysis. The apparent discrepancy between the IC_{50} and K_d values can be explained as below. The Hill coefficient of [^{3}H]15d-$\Delta^{12,14}$-PGJ_2 was less than 1, suggesting that there were several binding sites with different affinities. Because the specific binding of [^{3}H]15d-$\Delta^{12,14}$-PGJ_2 did not reach saturation in the Scatchard plot, there were two binding sites of [^{3}H]15d-$\Delta^{12,14}$-PGJ_2 with low and high affinities for 15d-$\Delta^{12,14}$-PGJ_2. 15d-$\Delta^{12,14}$-PGJ_2 appeared to induce neuronal cell death via the low-affinity binding site, but not the high-affinity binding site.

PGD_2 is one of the conventional eicosanoids, but it induced neuronal apoptosis as well as the cyclopentenone-type PGs, i.e., 15d-$\Delta^{12,14}$-PGJ_2. Does PGD_2 trigger apoptosis via GTP-binding protein-coupled PGD_2 receptors? This

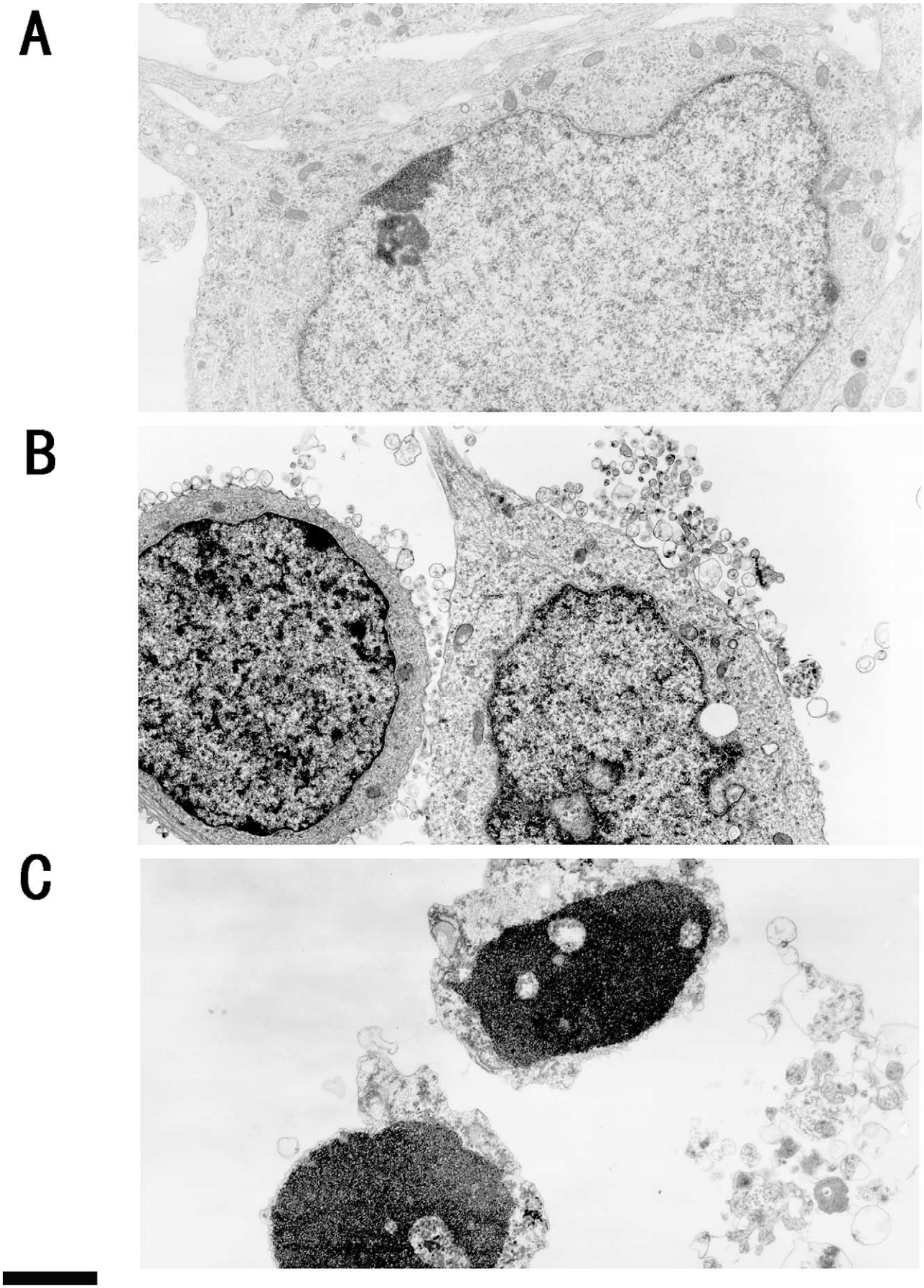

Fig. 13. Ultrastructural changes in cortical neurons by PGD_2 and 15-d-$\Delta^{12,14}$-PGJ_2. Cortical neurons were treated with vehicle (A), 10 μM PGD_2 (B), or 10 μM 15d-$\Delta^{12,14}$-PGJ_2 (C). The cultures were examined 12 h later by electron microscopy. Bar = 3 μm.

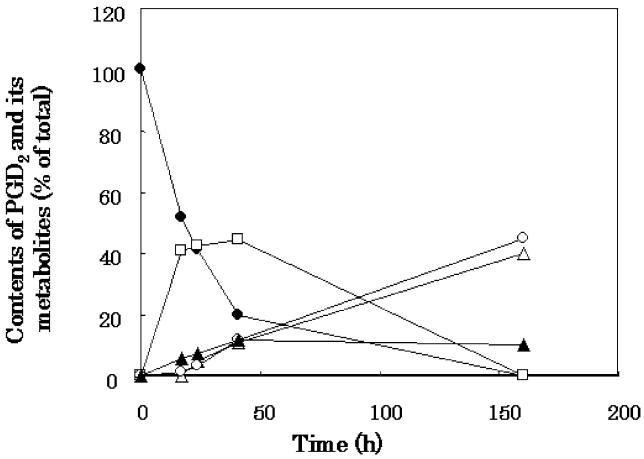

Fig. 14. Metabolism of PGD_2 in the culture medium. PGD_2-[^{3}H]PGD_2 was incubated in the serum-free culture medium at 37°C. At the indicated times, samples were withdrawn, acidified to pH 3 with formic acid, and extracted immediately with 3X 5 ml of ethyl acetate. The solvent was evaporated under nitrogen, and residual metabolites of [^{3}H]PGD_2 were quantitatively converted into its naphthacyl ester by reaction with α-bromoacetonaphtone and diisopropylethylamine in acetonitrile. The acetonitrile was evaporated, and the residue was reconstituted in chromatographic mobile phase containing glyceryl guiacholate, an internal standard for quantitation. PGD_2 (closed circles), PGJ_2 (open circles), Δ^{12}-PGJ_2 (open triangles), 15d-$\Delta^{12,14}$-PGJ_2 (open squares), and 15d-$\Delta^{12,14}$-PGD_2 (closed triangles).

possibility was not supported: First, the DP receptor blocker did not inhibit PGD_2-induced neuronal cell death. Second, little mRNA of the PGD_2 receptor is observed in the rat [26,27] and human [25] cerebral cortex. Third, few binding sites of [^{3}H]PGD_2 were detected in plasma membranes from cortices of rat and human (32). Fourth, the extent of specific [^{3}H]PGD_2 in total binding is much lower (30–40%) than that of [^{3}H] 15d-$\Delta^{12,14}$-PGJ_2 (>80%), although binding sites of PGD_2 have been reported in synaptosomes of rat [27] and human brains [33]. Fifth, the ED_{50} value (8.2 μM) of PGD_2 is much higher than the affinity for PGD_2 receptor [dissociation constant (K_d) = 28 nM] [27]. Finally, PGD_2 required a latent time to cause apoptosis. Thus, it is unlikely that PGD_2 causes neuronal cell death via the PGD_2 receptor.

PGD_2 was shown to be dehydrated to PGJ_2 in aqueous solution [30], and metabolized to 15-deoxy-$\Delta^{12,14}$-PGD_2 (15d-$\Delta^{12,14}$-PGD_2), Δ^{12}-PGJ_2, and 15d-$\Delta^{12,14}$-PGJ_2 in the presence of human albumin [4]. We confirmed that PGD_2 was nonenzymatically metabolized to 15d-$\Delta^{12,14}$-PGD_2, PGJ_2, Δ^{12}-PGJ_2, and 15d-$\Delta^{12,14}$-PGJ_2 in serum-free culture medium. In the present culture, PGJ_2, Δ^{12}-PGJ_2, and 15d-$\Delta^{12,14}$-PGJ_2 caused neuronal cell death without a latent time. Among the PGJ_2 series, 15d-$\Delta^{12,14}$-PGJ_2 induced neuronal cell death most potently and rapidly. The process of neuronal cell death induced by PGD_2 showed apoptotic features such as progressive cell shrinkage, blebbing of the plasma membrane, clumping of chromatin, and fragmentation of DNA. These apoptotic features were similar to those of 15d-$\Delta^{12,14}$-PGJ_2-treated neurons. Taken together with previous reports, the present study indicated that PGD_2 induced apoptosis via its metabolites, especially 15d-$\Delta^{12,14}$-PGJ_2, in neurons.

J-series PGs, including 15d-$\Delta^{12,14}$-PGJ_2, induce apoptosis in tumor cells [10]. In proliferative cells, 15d-$\Delta^{12,14}$-PGJ_2 arrests the progression of the cell cycle, inhibits the growth of tumors, and initiates an irreversible apoptotic pathway. How does 15d-$\Delta^{12,14}$-PGJ_2 induce apoptosis in nonproliferative cells such as differentiated neuronal cells? Independently of PPARγ, 15d-$\Delta^{12,14}$-PGJ_2 generates reactive oxygen species and induces apoptosis of human hepatic myofibroblasts [12]. Previously, we have reported that reactive oxygen species mediate apoptosis by neurotoxins such as amyloid-β proteins [34,35], suggesting a novel mechanism that involves oxidative stress and is related to the cell surface binding sites of 15d-$\Delta^{12,14}$-PGJ_2. Further studies are required to elucidate how the novel binding sites of 15d-$\Delta^{12,14}$-PGJ_2 is involved in neuronal apoptosis.

Recently, it has been reported that 15d-$\Delta^{12,14}$-PGJ_2 is involved in neurologic diseases such as sporadic amyotrophic lateral sclerosis [36]. Furthermore, its precursor, PGD_2, is increased significantly in several neurologic diseases such as Alzheimer's disease (AD) [37] and stroke [38]. AD is characterized clinically by progressive dementia and pathologically by cortical atrophy, neuronal loss, neurofibrillary tangles, senile plaques, and vascular deposits of amyloid-β protein (Aβ) in various regions of the cerebral cortex and the hippocampus. Aβ is a 39- to 43-amino-acid hydrophobic peptide, and Aβ-induced neuronal cell death is typified by several characteristic features of apoptosis, such as formation of cell surface blebs, chromatin condensation, and DNA fragmentation [21,39]. Aβ causes peroxidation of the plasma membrane [34,35], activation of L-type voltage-dependent calcium channels, and elevation of the intracellular Ca^{2+} level ([Ca^{2+}]i) [35,39–42]. The resulting increase in [Ca^{2+}]i activates phospholipase A_2 (PLA_2), which will release AA from the membrane. Recently, we have reported that Aβ generated PGD_2 before neuronal cell death [39].

Stroke is caused by an acute obstruction of arteries, resulting in ischemia, i.e., insufficient blood flow. Several inflammatory factors, including $sPLA_2$-IIA and eicosanoids such as PGD_2, are increased in the MCA-occluded rat brain [43]. Recently, we have established $sPLA_2$-IIA-induced neuronal cell death as an in vitro model for stroke [23]. $sPLA_2$-IIA potentiates Ca^{2+} influx into neurons via L-type voltage-sensitive calcium channels [44]. We have reported that $sPLA_2$-IIA generated PGD_2 from neurons before neuronal cell death. Thus, PGD_2 appears be involved in the neuronal cell death of AD and stroke via the novel binding sites of 15d-$\Delta^{12,14}$-PGJ_2.

In conclusion, we demonstrated that novel binding sites of 15d-$\Delta^{12,14}$-PGJ_2 exist on the cell surface of cortical neurons. 15d-$\Delta^{12,14}$-PGJ_2 induces neuronal apoptosis independently of PPARγ. We suggest that the novel binding

sites of 15d-$\Delta^{12,14}$-PGJ_2 might be involved in 15d-$\Delta^{12,14}$-PGJ_2-induced neuronal apoptosis.

Acknowledgment

The authors thank to Dr. Hitoshi Arita for his guidance and valuable discussions.

References

[1] P. Needleman, J. Turk, B.A. Jakschik, A.R. Morrison, J.B. Lefkowith, Arachidonic acid metabolism, Annu. Rev. Biochem. 55 (1986) 69–102.

[2] M. Negishi, T. Koizumi, A. Ichikawa, Prostanoid receptors and their biological actions, Prog. Lipid. Res. 32 (1993) 417–434.

[3] K. Ohno, T. Sakai, M. Fukushima, S. Narumiya, M. Fujiwara, Site and mechanisms of growth inhibition by prostaglandins. IV. Effect of cyclopentenone prostaglandins on cell progression of G1-enriched Hela S3 cells, J. Pharmacol. Exp. Ther. 245 (1988) 294–299.

[4] F.A. Fitzpatrick, M.A. Wynalda, Albumin-catalyzed metabolism of prostaglandin D_2, J. Biol. Chem. 258 (1983) 11713–11718.

[5] B.M. Forman, P. Tontonoz, J. Chen, R.P. Brun, B.M. Spiegelman, R.M. Evans, 15-deoxy-$\Delta^{12,14}$-prostaglandin J_2 is a ligand for the adipocyte determination factor PPARγ, Cell 83 (1995) 803–812.

[6] S.A. Kliewer, J.M. Lenhard, T.M. Willson, I. Patel, D.C. Morris, J.M. Lehmann, A prostaglandin J metabolite binds peroxysome proliferator-activated receptor g and promotes adipocyte differentiation, Cell 83 (1998) 813–819.

[7] O. Braissant, F. Foufelle, C. Scotto, M. Dauca, W. Wahli, Differential expression of peroxisome proliferator-activated receptors (PPARs): tissue distribution of PPAR-alpha, -beta, and -gamma in the adult rat, Endocrinology 137 (1996) 354–366.

[8] T. Kainu, A.-C. Wikström, J.-Å. Gustafsson, M. Pelto-Huikko, Localization of the peroxisome proliferator-activated receptor in the brain, Mol. Neurosci. 5 (1994) 2481–2485.

[9] J. Auwerx, PPARγ, the ultimate thrifty gene, Diabetologia 42 (1999) 1033–1049.

[10] S.A. Kliewer, T.M. Willson, The nuclear receptor PPARgamma—bigger than fat, Curr. Opin. Genet. Dev. 8 (1998) 576–581.

[11] T.T. Rohn, S.M. Wong, C.W. Cotman, D.H. Cribbs, 15-Deoxy-$\Delta^{12,14}$-prostaglandin J_2, a specific ligand for peroxisome proliferator-activated receptor, induces neuronal apoptosis, NeuroReport 12 (2001) 839–843.

[12] L. Li, J. Tao, J. Davaille, C. Féral, A. Mallat, J. Rieusset, H. Vidal, S. Lotersztajn, 15d-$\Delta^{12,14}$-PGJ_2 induces apoptosis of human hepatic myofibroblasts, J. Biol. Chem. 276 (2001) 38152–38158.

[13] S. Vaidya, E.P. Somers, S.D. Wright, P.A. Detmers, V.S. Bansal, 15-deoxy-$\Delta^{12,14}$-prostaglandin J_2 inhibits the β_2 integrin-dependent oxidative burst: involvement of a mechanism distinct from peroxysome proliferator activated receptor γ ligation, J. Immunol. 163 (1999) 6187–6192.

[14] T. Yagami, Differential coupling of glucagon and β-adrenergic receptors with the small and large forms of the stimulatory G protein, Mol. Pharmacol. 48 (1995) 849–854.

[15] N.N. Aronson Jr., O. Touster, Isolation of rat liver plasma membrane fragments in isotonic sucrose, Methods. Enzymemol. 31 (1974) 90–102.

[16] A. Arimura, K. Yasui, J. Kishino, F. Asanuma, H. Hasegawa, S. Kakudo, M. Ohtani, H. Arita, Prevention of allergic inflammation by a novel prostaglandin receptor antagonist, S-5751, J. Pharmacol. Exp. Ther. 298 (2001) 411–419.

[17] T. Yagami, K. Ueda, K. Asakura, S. Hata, T. Kuroda, J. Kishino, T. Sakaeda, G. Sakaguchi, N. Itoh, Y. Hori, Group IB secretory phospholipase A_2 induces cell death in cultured cortical neurons: a possible involvement of its binding sites, Brain Res. 949 (2002) 197–201.

[18] K. Ueda, Y. Fukui, H. Kageyama, Amyloid β protein-induced neuronal cell death: neurotoxic properties of aggregated amyloid β protein, Brain Res. 639 (1994) 240–244.

[19] K. Ueda, T. Yagami, K. Asakura, K. Kawasaki, Chlorplomazine reduces toxicity and Ca^{2+} uptake induced by amyloid β protein (25–35) in vitro, Brain Res. 748 (1997) 184–188.

[20] T. Yagami, K. Ueda, K. Asakura, Y. Hayasaki-Kajiwara, H. Nakazato, T. Sakaeda, S. Hata, T. Kuroda, N. Takasu, Y. Hori, Group IB secretory phospholipase A_2 induces neuronal cell death via apoptosis, J. Neurochem. 81 (2002) 449–461.

[21] K. Ueda, T. Yagami, H. Kageyama, K. Kawasaki, Protein kinase inhibitor attenuates apoptotic cell death induced by amyloid β protein in culture of the rat cerebral cortex, Neurosci. Lett. 203 (1996) 175–178.

[22] T. Yagami, K. Ueda, K. Asakura, T. Sakaeda, G. Sakaguchi, N. Itoh, S. Hata, T. Kuroda, Y. Hashimoto, Y. Hori, Porcine group IB secretory phospholipase A_2 potentiates Ca^{2+} influx through L-type voltage-sensitive Ca^{2+} channel, Brain Res. 960 (2003) 71–80.

[23] T. Yagami, K. Ueda, K. Asakura, S. Hata, T. Kuroda, T. Sakaeda, N. Takasu, K. Tanaka, T. Gemba, Y. Hori, Human group IIA secretory phospholipase A_2 induces neuronal cell death via apoptosis, Mol. Pharmacol. 61 (2002) 1–13.

[24] T. Yagami, K. Ueda, K. Asakura, Y. Hori, Deterioration of axotomy-induced neurodegeneration by group IIA secretory phospholipase A_2, Brain Res. 917 (2001b) 230–234.

[25] K. Asakura, T. Kanemasa, K. Minagawa, K. Kagawa, M. Ninomiya, The nonpeptide α-eudesmol from Juniperus virginiana Linn. (Cupressaceae) inhibits ω-agatoxin IVA-sensitive Ca^{2+} currents and synaptosomal $^{45}Ca^{2+}$ uptake, Brain Res. 823 (1999) 169–176.

[26] Y. Boie, N. Sawyer, D.M. Slipetz, K.M. Metters, M. Abramovitz, Molecular cloning and characterization of the human prostanoid DP receptor, J. Biol. Chem. 270 (1995) 18910–18916.

[27] D.H. Wright, F. Nantel, K.M. Metters, A.W. Ford-Hutchinson, A novel biological role for prostaglandin D_2 is suggested by distribution studies of the rat DP prostanoid receptor, Eur. J. Pharmacol. 377 (1999) 101–115.

[28] T. Shimizu, A. Yamamoto, O. Hayaishi, Specific binding of prostaglandin D_2 to rat brain synaptic membrane, J. Biol. Chem. 257 (1982) 13570–13575.

[29] M. Fukushima, T. Kato, K. Ota, Y. Arai, S. Narumiya, O. Hayaishi, 9-deoxy-delta 9-prostaglandin D_2, a prostaglandin D_2 derivative with potent antineoplastic and weak smooth muscle-contracting activities, Biochem. Biophys. Res. Commun. 109 (1982) 626–633.

[30] T. Sasaguri, J. Masuda, K. Shimokado, T. Yokota, C. Kosaka, M. Fujishima, J. Ogata, Prostaglandins A and J arrest the cell cycle of cultured vascular smooth muscle cells without suppression of *c-myc* expression, Exp. Cell. Res. 200 (1992) 351–357.

[31] M.T. Heneka, T. Klockgether, D.L. Feinstein, Peroxisome proliferator-activated receptor-γ ligands reduce neuronal inducible nitric oxide synthase expression and cell death in vivo, J. Neurosci. 20 (2000) 6862–6867.

[32] D. Gerashchenko, C.T. Beuckmann, Y. Kanaoka, N. Eguchi, W.C. Gordon, Y. Urade, N.G. Bazan, O. Hayaishi, Dominant expression of rat prostanoid DP receptor mRNA in leptomeninges, inner segments of photoreceptor cells, iris epithelium, and ciliary processes, J. Neurochem. 71 (1998) 937–945.

[33] Y. Watanabe, H. Tokumoto, A. Yamashita, S. Narumiya, N. Mizuno, O. Hayaishi, Specific binding of prostaglandin D_2, E_2, $F_{2\alpha}$ in postmortem human brain, Brain Res. 342 (1985) 110–116.

[34] C. Behl, J.B. Davis, G.M. Cole, D. Scubert, Vitamin E protects nerve cells from amyloid β protein toxicity, Biochem. Biophys. Res. Commun. 186 (1992) 944–950.

[35] K. Ueda, S. Shinohara, T. Yagami, K. Asakura, K. Kawasaki, Amyloid β protein potentiates Ca^{2+} influx through L-type voltage-sensitive Ca^{2+} channels: a possible involvement of free radicals, J. Neurochem. 68 (1997) 265–271.

[36] M. Kondo, T. Shibata, T. Kumagai, T. Osawa, N. Shibata, M. Kobayashi, S. Sasaki, M. Iwata, N. Noguchi, K. Uchida, 15-Deoxy-$\Delta^{12,14}$-prostaglandin J_2: the endogenous electrophile that induces neuronal apoptosis, Proc. Natl. Acad. Sci. USA 99 (2002) 7367–7372.

[37] N. Iwamoto, K. Kobayashi, K. Kosaka, The formation of prostaglandins in the postmortem cerebral cortex of Alzheimer-type dementia patients, J. Neurol. 236 (1989) 80–84.

[38] R.J. Gaudet, I. Alam, L. Levine, Accumulation of cyclooxygenase products of arachidonic acid metabolism in gerbil brain during reperfusion after bilateral common carotid artery occlusion, J. Neurochem. 35 (1980) 653–658.

[39] T. Yagami, K. Ueda, K. Asakura, T. Sakaeda, T. Kuroda, S. Hata, Y. Kambayashi, M. Fujimoto, Effects of S-2474, a novel nonsteroidal anti-inflammatory drug, on amyloid β protein-induced neuronal cell death, Br. J. Pharmacol. 134 (2001) 673–681.

[40] T. Yagami, K. Ueda, K. Asakura, T. Kuroda, S. Hata, T. Sakaeda, Y. Kambayashi, M. Fujimoto, Effects of endothelin B receptor agonists on amyloid β protein-induced neuronal cell death, Brain Res. 948 (2002) 72–81.

[41] T. Yagami, K. Ueda, K. Asakura, T. Sakaeda, Y. Kambayashi, G. Sakaguchi, N. Itoh, Y. Hashimoto, H. Tsuzuki, Effect of PGE_2 on amyloid β protein-induced neuronal cell death, Brain Res. 959 (2003) 328–335.

[42] T. Yagami, K. Ueda, K. Asakura, T. Sakaeda, G. Sakaguchi, N. Itoh, S. Hata, T. Kuroda, Y. Kambayashi, H. Tsuzuki, Effect of Gas6 on amyloid β protein-induced neuronal cell death, Neuropharmacology 43 (2002) 1289–1296.

[43] K. Umemura, H. Kawai, H. Ishihara, M. Nakashima, Inhibitory effect of clopidogrel, vapiprost and argatroban on the middle cerebral artery thrombosis in the rat, Jpn. J. Pharmacol. 67 (1995) 253–258.

[44] T. Yagami, K. Ueda, K. Asakura, T. Sakaeda, H. Nakazato, S. Hata, T. Kuroda, G. Sakaguchi, I. Itoh, Y. Hashimoto, Y. Hori, Human group IIA secretory phospholipase A_2 potentiates Ca^{2+} influx through L-type voltage-sensitive Ca^{2+} channel, J. Neurochem. 85 (2003) 749–758.